

ELECTRON CLOUD EFFECTS IN THE J-PARC RINGS AND RELATED TOPICS

T. Toyama* and the e-cloud study team, KEK, Tsukuba, Japan

Abstract

Electron build-up and collective beam instabilities in the J-PARC rings has been expected by simulation. Bunched beam parameters are close to instability threshold. Coasting beam is stable at the nominal parameter. One of implications is that J-PARC is not in saturation regime, which suggests that keeping the source of electrons, i.e. beam losses, less than a critical value is effective to reduce the electron cloud density. Controlled beam losses are reviewed and confirm the losses are less than the limit. At the KEK PS electron clouds in bunched and coasting beams are observed with the electron-sweeping detector developed at LANL. The results are consistent with the behavior previously reported from LANL.

INTRODUCTION

J-PARC [1] is a Japan Proton Accelerator Research Complex as a joint project of KEK and JAERI. Construction is in progress and commissioning is scheduled to start from 2007. J-PARC equips two circular proton accelerators: one is a 3 GeV rapid cycling synchrotron (RCS) and the other is a 50 GeV proton synchrotron (MR). RCS is used as a source of neutrons and mesons, and as an injector to MR. It accelerates proton beams from 400 MeV (180 MeV in phase I) to 3 GeV at the repetition rate of 25 Hz. MR is used for experiments of nuclear physics and neutrino physics. It accelerates the beam up to 50 GeV and supply with fast and slow extraction. In the slow extraction, coasting beam operation is adopted. The parameters of the two rings are summarized in Table 1. The bunch structure, the population of 4×10^{13} and the length of 16-110 m, is comparable with PSR. Therefore electron cloud effect may affect the accelerator performance. The electron cloud effect has been studied by computer simulations and investigated by experiments at the KEK 12 GeV PS.

SIMULATION STUDIES

Instability for bunched beams in the RCS and MR^[2]

Electron cloud build-up is estimated by analyzing motion of electrons produced at the chamber wall due to primary and secondary productions. We assume that primary electrons are produced at the chamber wall with a yield per traveling of 1 m of a proton, $Y_1 = 4 \times 10^{-6}$ e/(m.p).

The secondary emission yield $\delta_2(E)$, which is the number of electrons created by an electron incidence with energy E , is approximated by Eq. (1),

Table 1: Parameters of J-PARC proton synchrotrons

		RCS		MR	
		inj.	ext.	inj.	ext.
Circumference	(m)	348.3	348.3	1567.5	1567.5
gamma		1.43	4.20	4.20	54.29
bunch population	E+13	4.15	4.15	4.15	4.15
Number of bunches		2	2	8	8
harmonic number		2	2	9	9
beam size	(m)	0.019	0.012	0.011	0.0035
bunch length	(m)	110	82	82	16
momentum spread	(%)	0.6	0.7	0.7	0.25
slippage factor		-0.48	-0.047	-0.058	-0.0013
synchrotron tune		0.0058	0.0005	0.0026	0.0001
beam pipe radius	(cm)	12.5	12.5	6.5	6.5

$$\delta_2(E) = \delta_{2,\max} \times \frac{E}{E_{\max}} \frac{1.44}{0.44 + (E/E_{\max})^{1.44}} \quad (1)$$

where $E_{\max} = 200$ eV, $\delta_2(0) = 0$ and $\delta_{2,\max} = 2.1$ are assumed. Improved simulation including electron's elastic reflection and space charge force between electrons shows a little change from this calculation [3].

Electron density at build up is obtained by tracking the electrons with the primary yield and by estimating the amplification due to secondary emission. The neutralization factor, defined by electron line density divided by bunch average line density, is shown in Table 2. In the table, the neutralization factors at peak and bottom densities due to bunch induced multipacting are written.

Instability threshold is estimated by coasting beam approximation. The approximation is reliable, because of $\omega_e \sigma_z / c \sim 100 \gg 1$. The threshold of the neutralization factor η is shown in Table 2.

Table 2: Amplification and neutralization factors. $\delta_2(0) = 0.5$ is assumed.

	RCS inj.	RCS ext.	MR inj.	MR ext.
Ae(bottom)	17	18	5.1	1.7
Ae(peak)	50	68	115	9.5
η (bottom)	0.022	0.0063	0.0028	0.0001
η (peak)	0.0075	0.022	0.063	0.0006
η (threshold)	0.28	0.03	0.03	0.00043

The neutralization factor is close to the threshold in every case at the peak density except for injection of RCS. The electron cloud gets to the peak density at the tail of bunch. MR is more serious than RCS, because of the low slippage factor. The primary yield, $Y_1 = 4 \times 10^{-6}$ e/(m.p), is used in all cases. The yield has been estimated in detail

* takeshi.toyama@kek.jp

according to the cases. The neutralization factor strongly depends on the secondary yield, $\delta_{2,\max}$. The value 2.1 is given for stainless steel with a conditioning, but it may be more 2.5~3 at the early stage of commissioning. In this case the neutralization factor exceeds the threshold value. To make easy the commissioning program, cures for example, TiN coating, is indispensable.

Instability for coasting beams at the MR

A coasting beam operation is planned for slow extraction in the 50 GeV main ring. The neutralization factor of the threshold is extremely low for the top energy of the MR as is shown in Table 2, because of the low slippage factor. If electrons created by ionization were just trapped, their density would reach the threshold value with a short time, 0.2 ms for a vacuum pressure of 2×10^{-7} Pa ($Y_1 = 8 \times 10^{-9}$ e/(m.p)). Considering the transverse momentum conservation, electrons whose density is 0.4% of proton beam are strongly swung by small perturbation of the proton beam. How the instability is observed actually depends on production rate of the electrons, namely the beam flicks the electrons immediately if they are accumulated up to the threshold value. The simulation of motion of the proton beam and electrons was performed [4], and showed that the beam amplitude does

not grow to visible level for such low production rate of electrons $Y_1 = 8 \times 10^{-9}$ e/(m.p).

On the other hand, electrons created at the chamber wall are produced by higher rate, typically $Y_1 = 4 \times 10^{-6}$ e/(m.p) as is discussed for bunched beams. A simulation was carried out for interaction between a coasting beam and electrons produced at the chamber, and shows that the beam amplitude grew to visible value for such high production rate. The results mean that electrons produced at the chamber wall with high rate were essential even for the instability of coasting beam.

BEAM LOSS CONSIDERATION

The simulation with J-PARC parameters shows that the electron cloud build-up is not in saturation regime [3]. It means less beam loss produces less equilibrium electron cloud density, and then reducing the beam loss and suppressing the electrons from those protons are worth the effort.

The expected beam losses are summarized in Table 3. The electrons from controlled beam loss will be suppressed with solenoid magnets or an electron catcher (for the carbon foil). We may say the beam is stable, if the electron production rate from the uncontrolled beam losses is smaller than the one corresponding to 4×10^{-6} e/m.p.

Table 3: Electrons due to beam losses in the RCS and the MR

		Proton loss	electron yield	Power	Cure
RCS	Charge exchange carbon foil	-	$1.7 \times 10^{14} / 500 \mu s$	140 W (electron)	electron catcher
	Second stripping foils H^0	-	$5 \times 10^{11} / 500 \mu s$	< 400 W (proton)	-
	H^-	-	-	-	-
	Halo collimator 181 MeV	$< 5.5 \times 10^{12}$	$5.5 \times 10^{14} / 500 \mu s$	< 4 kW (proton)	solenoid
	400 MeV	$< 2.5 \times 10^{12}$	$2.5 \times 10^{14} / 500 \mu s$	-	solenoid
MR	Uncontrolled loss 181 MeV	$< 1.1 \times 10^{11}$	1.1×10^{13}	-	-
	400 MeV	$< 5 \times 10^{10}$	5×10^{12}	-	-
	Halo collimator controlled loss	$< 6.6 \times 10^{11} \times 5$	$6.6 \times 10^{13} \times 5$	450 W (pr)	solenoid

Electron yields are estimated using the assumption that one proton produces 100 electrons [5]. All controlled losses are assumed to occur at the multi-turn injection period of $500 \mu s$ in the RCS and suppressed with an electron catcher and the solenoid windings. Two percent of stored beam will be lost as an uncontrolled losses during halo collimation. This will occur, at least, within the injection period of $500 \mu s$. Normalizing the number of electrons by the circumference and the number of protons, the electron production rate comes to 1.6×10^{-6} e/m.p (0.6×10^{-6} e/m.p) at 400 MeV (181 MeV).

In the MR 0.2% of the injected beam can be collimated at the maximum. Almost all of the scattered particles will be caught in the collimator area, accounting only primary scattering. If solenoid windings suppress the electron build-up in the collimator area, the electrons may have no

effects in the MR. Secondary and tertiary scattering will be included in the study of next stage [1].

Both of the production rate are less than 4×10^{-6} e/m.p and the beam may be stable. The normalization by the ring circumference used in calculating the electron production rate may be correct as far as the electron cloud build-up is not in the saturation regime.

The stability criterion includes ambiguities in each process, the proton-induced electron-production rate, cloud build-up rate and instability dynamics, moreover those processes might correlate. These points will be studied in future.

The halo collimator design is in further progress. From the practical point of view, TiN coating will be performed in the collimators and other modifications are proceeding.

EXPERIMENTS AT THE KEK-PS

The observation of electron clouds at the Main Ring (MR) of the KEK-PS is going on to benchmark the computer simulation and to test materials such as TiN coating on stainless steel and alumina ceramic pipes. The scaled version of electron sweeping detector developed by the LANL team [6] was recently installed in the ring. The KEK-PS MR accelerates nine proton bunches from 500 MeV to 12 GeV. The parameters of the ring are summarized in Table 4.

Table 4: Parameters of KEK 12 GeV PS

		MR	
		injection	extraction
Circumference (m)		339.3	339.3
gamma		1.53	13.8
bunch population		$\leq 9 \text{ E}+11$	$\leq 9 \text{ E}+11$
Number of bunch		≤ 9	≤ 9
harmonic number		9	9
beam size (rms)* (m)		$\sim 0.005/\sim 0.007$	$\sim 0.002/\sim 0.003$
bunch length (m)		~ 20	~ 18
momentum spread (%)		0.4	0.4
slippage factor		-0.40	0.017
synchrotron tune		~ 0.008	0.0004
beam pipe radius* (cm)		~ 6	~ 6

*) Value estimated at the position of the e-sweeping detector.

Observation of bunched beams

Previous observation indicated the existence of electron clouds for bunched beams at the phase transition (~ 5.3 GeV) and the flat top energy (12 GeV) [7]. Recent observation shows concrete evidence of the electron clouds. Collective beam instabilities are not observed due to electron clouds so far.

The electron sweeping detector comprises slits, a grid, a collector and a HV plate as shown in Fig. 1.

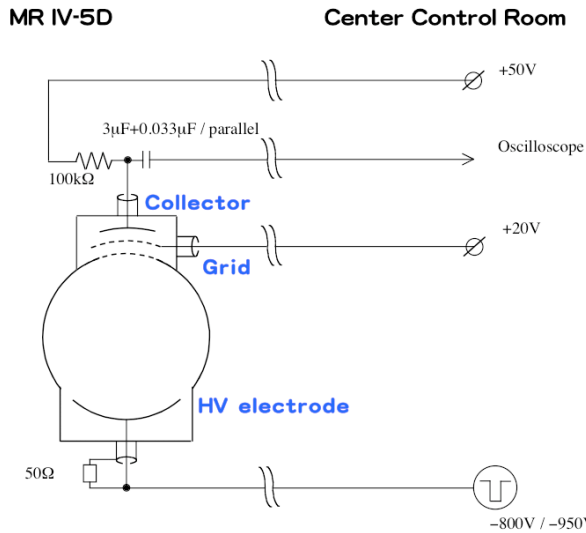


Figure 1: Electron sweeping detector at the KEK-PS Main Ring.

The typical signals from the collector without sweeping voltage are shown in Figs. 2 and 3. Upper plots are the signals from the collector. Lower plots are the signals from a wall current monitor just downstream of the e-sweeping detector. The accumulation of electrons is clearly seen, comparing the collector signals of two different number of bunches, nine and six. There are no collector signals less than or equal to 5 bunches.

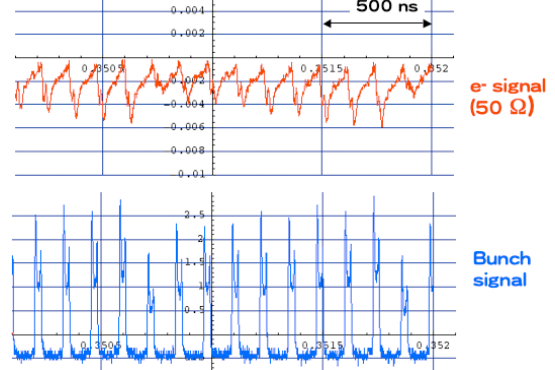


Figure 2: Signals from the collector and wall current monitor for nine bunches.

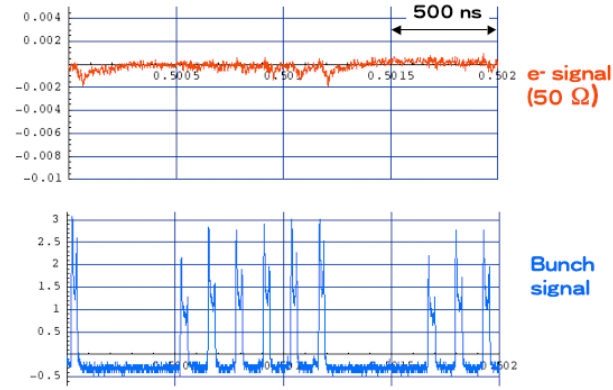


Figure 3: Signals from the collector and wall current monitor for six bunches.

With a HV pulse of 50 ns, 850V (at the output of the pulser), a large signal was detected as Fig. 4. Just after sweeping the electrons, the electron signal is reduced and gradually increasing within a few bunch passages, which is similar to that observed at LANL [6].

Observation of coasting beams

A model that assumes continuous ionization of a residual gas by the proton beam, diffusion of electrons and multipacting due to beam oscillation is described in the previous section. It predicts saturation of electron cloud density. The goal of the experiments is to confirm the above picture. The result of an experiment with the e-sweeping detector is shown in Fig. 5: electron cloud build-up for several coasting beam intensities and with artificial beam loss.

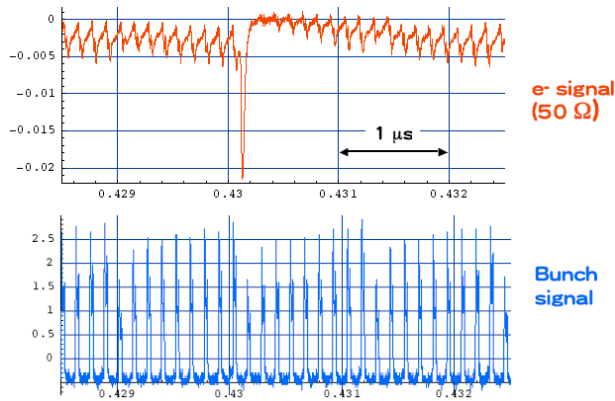


Figure 4: Signals from the collector and wall current monitor for nine bunches. A large electron signal around the middle of the trace corresponds to the HV sweeping pulse.

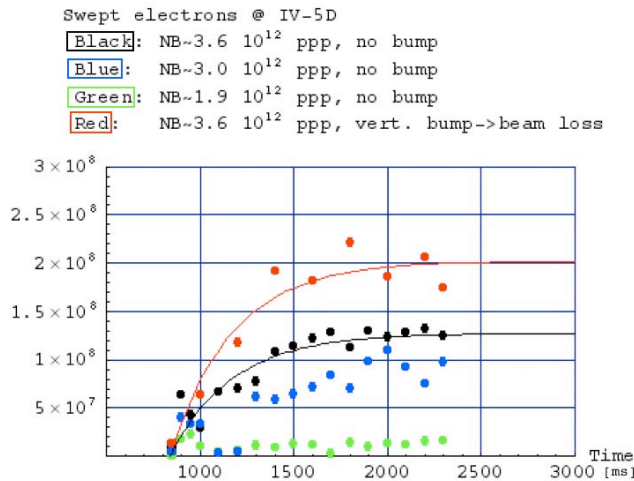


Figure 5: Number of electrons swept out with HV (~ -850 V, 100 ns) after a time from the acceleration starting trigger. RF is turned off at ~ 850 ms.

Using the following expression for electron cloud build-up:

$$\mu\tau(1 - e^{-t/\tau}), \quad \tau : \text{decay constant [s]}, \\ \mu : \text{production rate [e}^-/\text{m}\cdot\text{s]},$$

we obtain the production rate of 1×10^{10} e/m/s and decay constant of 0.3 s for the beam intensity of 3.6×10^{12} ppp. Saturated electron density is 3×10^9 e/m, assuming detector efficiency of 0.04, which is the ratio of the number of ejected electrons from the beam pipe to the detector, and the number of electrons in the pipe volume of one meter in the beam direction. The local neutralization factor is $\sim 30\%$.

With the artificial beam loss, the production rate increased by 60% comparing to the above case. The loss amount was so small that an air-filled loss monitor could not detect it and only a scintillation counter did detect.

Reducing the beam intensity caused rapid decrease of the electron cloud density.

CONCLUSION

Using the J-PARC beam parameters, electron cloud build-up and collective beam instabilities are simulated for bunched and coasting beams. The bunched beams at the extraction of the 3 GeV RCS and at the injection and extraction of the 50 GeV MR are close to the instability threshold, assuming $\delta_{2,\max}=2.1$ and $\delta_2(0)=0.5$. The inner surface of the ceramic pipe of the 3 GeV RCS will be coated by TiN, which will drastically suppress the electron cloud build-up due to smaller secondary electron yield [2]. The SEY suppression depends on the coating process [8]. We plan to make TiN coating samples with the same process for mass production, install it in the KEK-PS electron-sweeping detector and check the electron yield.

Another important issue is to examine the beam loss at each stage of acceleration. The above calculation relies on the beam loss rate of $Y_1=4 \times 10^{-6}$ e/(m.p) and primary electron production rate of ~ 100 e/p. Less amount of beam losses causes smaller electron density and more amount of beam losses more electron density [3], which means that the electron density is not saturated in J-PARC. Reducing an amount of losses is important. Preliminary estimate at each acceleration stages shows smaller losses than the one above mentioned. We will pursue better accuracy of prediction, follow up an improving design of collimators and try to keep the beam loss small.

The measurements using the electron sweeping detector at the KEK-PS shows the existence of the electron cloud both in the bunched and coasting beams. Comparing the results to the simulation is foreseen.

ACKNOWLEDGEMENTS

The author wishes to thank S. Machida, K. Ohmi, K. Oide, G. Rumolo, K. Satoh, K. Yokoya and F. Zimmermann for theoretical aspects; N. Hayashi, S. Igarashi, Y. Irie, S. Kato, T. Kubo, T. Miura, C. Ohmori, Y. Saito, Y. Sato, M. Shirakata, M. Tomizawa and M. Uota for experiments and vacuum aspects; and R. Macek for providing information on the electron detector.

REFERENCES

- [1] "Accelerator Technical Design Report for J-PARC" edited by Y. Yamazaki, KEK-report 2002-13.
- [2] K. Ohmi, T. Toyama, C. Ohmori, PRST-AB **5**, 114402 (2002).
- [3] http://www-acpps.kek.jp/JPARC/beam_instability/epi_ohmi_2002Jun12.pdf.
- [4] K. Ohmi, T. Toyama and M. Tomizawa, Proc. PAC03 (2003). K. Ohmi, these proceedings.
- [5] P. Thieberger et al., Phys. Rev. **A61**, 042901 (2000). The results in this reference do not include one that corresponds the J-PARC energy, hence the round number is used in the text.
- [6] R. J. Macek, Proc. ELOUD'02 workshop, CERN Yellow Report, CERN-2002-001, p. 259 and references therein. The radial dimension was scaled up as an inner radius from 5 cm to 8 cm.
- [7] T. Toyama et al., Proc. ELOUD'02 workshop, CERN Yellow Report, CERN-2002-001, p. 155.
- [8] Y. Saito, private communication.